ChemComm

Accepted Manuscript

This article can be cited before page numbers have been issued, to do this please use: X. Yang, W. liu, J. tang, P. Li, H. weng, Y. Ye, M. Xian, B. Tang and Y. F. Zhao, *Chem. Commun.*, 2018, DOI: 10.1039/C8CC05418E.

ROYAL SOCIETY OF CHEMISTRY

rsc.li/chemcomm

View Article Online
DOI: 10.1039/C8CC05418E

Journal Name

ARTICLE

A multi-signal mitochondria-targeted fluorescent probe for real-time visualizing cysteine metabolism in living cells and animals

Received 00th January 20xx,
Accepted 00th January 20xx

DOI: 10.1039/x0xx00000x

www.rsc.org/

Xiaopeng Yang[a], Wenya Liu[a], Jun Tang[a], Ping Li[b], Haibo Weng[c]*, Yong Ye[a]*, Ming Xian[d], Bo Tang[b] and Yufen Zhao[a]

In this study, we developed a multi-signal mitochondria-targeted fluorescent probe (NIR-Cys) for simultaneous detection of Cys and its metabolite, SO_2. In the design of the probe, the acrylate group and C=C of coumarin ring were used as the recognizing moiety for Cys and SO_2, respectively. The probe exhibited high sensitivity, excellent specificity, and fast response. NIR-Cys was found to precisely target and visualize Cys metabolism in mitochondria of living cells with multi-fluorescent signal. This probe is expected to be a useful tool for understanding Cys metabolism.

As the only mercapto (-SH) containing amino acid, cysteine (Cys) plays crucial roles in a wide variety of physiological and pathological processes such as protein synthesis, signal transduction, post-translational modification, diverse redox chemistry, and metabolism[1-3]. For instance, abnormal concentrations of Cys can lead to various diseases[4-7], including liver damage, neurotoxicity, hematopoiesis, skin lesions, slowed growth, Alzheimer's, and Parkinson's. It has been reported that metabolic pathways of Cys can be divided into two types[8]. One is the cysteine sulfinate pathway that Cys is oxidized by cysteine dioxygenase (CDO) to form cysteinesulfinate, and then enzymatically translates to β-sulfinylpyruvate, through transamination by aspartate aminotransferase (AAT). β-Sulfinylpyruvate spontaneously decomposes to SO_2 and pyruvate. The other is the desulfuration metabolism that Cys undergoes 3-mercaptopyruvate pathway in mitochondria without initial oxidation of the sulfur atom (Scheme 1A). Although the research on Cys metabolism has received attention[9], simple visualization methods for monitoring the process are still lacking. Molecular imaging technology based on fluorescent probes can enable visualization of biologically relevant species in cells, tissues and organisms, and can provide useful information about the biological effects of the analytes[10]. Owing to their high sensitivity and simplicity, fluorescent probes have been widely used to monitor biomolecules as well as to visualize metabolic processes[11]. Recently, some fluorescent probes for separate detection of Cys and SO_2 have been developed[12], but few probes achieved the visualization of Cys metabolism. For example, Yin et al. reported a fluorescent probe for real-time visualizing Cys in living A549 cells[13]. But Yin's probe cannot be used to detect both Cys and SO_2. Zhang et al. reported a ratiometric fluorescent probe for SO_2 detection in hepatic BRL cells. However, Zhang's probe cannot be used to detect Cys[14]. As such, fluorescent probes that can directly visualize cysteine-SO_2 metabolism with high accuracy and resolution using multi-fluorescence signals are urgently needed. Those probes will be crucial in understanding the roles of cysteine metabolism in physiological and pathological conditions.

Mitochondria are "power house" and the main source of reactive sulfur species (RSS) and reactive oxygen species (ROS) [15]. As a vital antioxidant reservoir to regulate ROS homeostasis, Cys is always presented in mitochondria. Under oxidative stress, Cys may be converted to SO_2. But detailed mechanism and process are still unclear. In addition, Cys plays a major role in mitochondrial protein turnover. Therefore, to obtain detailed information on Cys metabolism in mitochondria, the development of fluorescent imaging for real-time observing Cys metabolism in living cells is very essential. To the best of our knowledge, fluorescent probes that allow direct detection of Cys-SO_2 metabolism in mitochondria have not been reported.

To fulfil this gap, herein we report a multi-signal fluorescent probe for real-time monitoring cysteine-SO_2 metabolism in mitochondria of living cells and animals (Scheme 1B). In the design of our probe, acrylate group was selected as the recognizing moiety for Cys. The reaction between Cys and acrylates results a conjugate addition to produce thioethers, and then an intramolecular cyclization to release the fluorophore NIR-OH. Meanwhile, sulfite can add to the C=C of coumarin ring via a unique nucleophilic addition, and the fluorescence signal should change from red to green which is dominated by the left benzopyran structure. If Cys and SO_2 co-exist, the response at different wavelengths should be observed. As expected, the probe showed high sensitivity, excellent selectivity, and rapid responses for Cys and SO_2. It has been successfully employed in real-time monitoring Cys metabolism in vivo. As shown in Scheme S1, NIR-Cys was synthesized from

[a] College of Chemistry and Molecular Engineering, Zhengzhou University, Zhengzhou 450001, China. E-mail: yeyong03@tsinghua.org.cn
[b] College of Chemistry, Key Laboratory of Molecular and Nano Probes, Ministry of Education, Shandong Normal University, Jinan 250014 , China.
[c] School of Life Science, Zhengzhou University, Zhengzhou 450001, China.
[d] Department of Chemistry, Washington State University, Pullman, WA 99164, USA.
† Footnotes relating to the title and/or authors should appear here.
Electronic Supplementary Information (ESI) available: [details of any supplementary information available should be included here]. See DOI: 10.1039/x0xx00000x

View Article Online
DOI: 10.1039/C8CC05418E

coumarin in three steps with excellent yields. The probe was fully characterized by ^{1}H NMR, ^{13}C NMR and HR-MS.

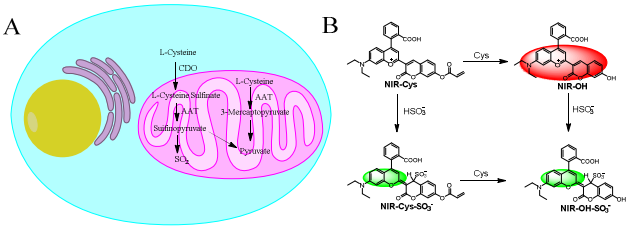

Scheme 1. (A) Metabolic pathways of Cys in mitochondria. (B) Design of the fluorescent probe for real-time visualizing Cys-SO_2 metabolism.

With the probe in hand, its spectroscopic performance was evaluated in HEPES buffer (pH= 7.4, 10 mM). As shown in Figure S1, the probe itself exhibited a central absorption at 570 nm and emission maximum at 656 nm with weak fluorescence. Upon the addition of 10 equiv. Cys, a new maximum absorption peaks red shift to 620 nm, and the fluorescence intensity at 656 nm increased significantly. Time-dependent responses of NIR-Cys showed that the reaction between the probe (10 μM) and 10 equiv. of Cys completed within 10 min (Figure 1A, inset). The fluorescent titration of NIR-Cys toward Cys at low concentrations were conducted and the detection limit (Figure S2) was calculated to be 30 nM (according to the 3σ/slope), which appeared to be sensitive than the reported Cys probes[12d,16]. The pH effect on fluorescence property of NIR-Cys (10 μM) toward Cys (100 μM) was also investigated. The fluorescence intensities were all obviously increased at 656 nm in the range of pH 7−10 (Figure S3). Those results indicated that NIR-Cys was suitable for real-time imaging Cys in real samples.

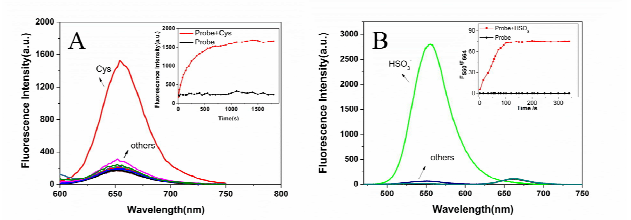

Figure 1. (A) The fluorescence intensity of NIR-Cys (10 μM) with Cys (10 equiv.) and other biologically relevant species (10 equiv.). (Including: NIR-Cys, SO_4^{2-}, $S_2O_3^{2-}$, $S_2O_8^{2-}$, NO_3^-, NO_2^-,Ser, Hcy, 5 mM GSH, ClO^-, ClO_4^-, H_2O_2, O_2^-, $^1O_2$, ·OH, Na^+, Zn^{2+}, Ca^{2+}, Ba^{2+}, Cu^{2+}, Fe^{2+}, Mn^{2+}, Pb^{2+}, Hg^{2+}, Sn^{2+}, Al^{3+}) (B) The fluorescence intensity of probe NIR-OH (10 μM) with HSO_3^- (10 equiv.) and other biologically relevant species (10 equiv.).(Including: NIR-OH, F^-, Cl^-, Br^-, I^-, CO_3^{2-}, HCO_3^-, ClO^-, ClO_4^-, AcO^-, PO_4^-, HPO_4^-, $H_2PO_4^-$, $S_2O_3^{2-}$, $S_2O_8^{2-}$, NO_3^-, NO_2^-, SO_4^{2-}, HS^-, SO_4^{2-}, Cys, Hcy, GSH).

We next evaluated the selectivity and interference of NIR-Cys for Cys detection. In this study, the probe was incubated with biologically relevant species such as amino acids (Figure S4), different ROSs, RSSs and ions (Figure 1A). The probe only showed slight fluorescence increase at 656 nm in the presence of these interfering analytes (Figure S5). In contrast, fluorescence intensity at 656 nm significantly increased upon the addition of Cys (100 μM). Furthermore, competitive experiments indicated that other species had no interference for Cys detection. Thus, the probe has the potential to detect Cys with excellent selectivity in complex biological environments. To confirm the sensing mechanism, the reaction product was characterized by mass spectrometry. A dominant peak at m/z 482.1601 was attributed to NIR-OH. The proposed sensing mechanism is shown in Scheme S2 based on the MS analysis (Figure S6) and previous literature[17].

We also found that NIR-Cys could react with HSO_3^-rapidly (50 s) (Figure S7B). After treating with HSO_3^- (100 μM), a new absorption peak at 470 nm emerged, accompanied with the peaks at 350 and 620 nm gradually decreased as shown in Figure S8. The probe NIR-Cys alone displayed weak fluorescence emission at 560 nm. However, the addition of HSO_3^-into the solution of NIR-Cys led to a distinct fluorescence increase at 560 nm (Figure S7A). The detection limit for HSO_3^- based on the 3σ/slope was 11.0 nM (Figure S9). The HSO_3^- sensing mechanism was also confirmed by MS as shown in Scheme S3 and Figure S10. A dominant peak at m/z 616.1306 was attributed to NIR-cys-SO_3. It should be noted that although the probe NIR-Cys can reacts with HSO_3^-, the level of Cys is much higher than that of HSO_3^- in living cells[4,13]. So NIR-Cys can detect Cys with high selectivity and generate NIR-OH, which can then monitor the level of SO_2 in the process of Cys metabolism.

NIR-OH is the intermediate produced from the probe (NIR-Cys) reacting with Cys. We next investigated its spectroscopic properties. As shown in Figure S11A, the maximum absorption peak was moved from 620 to 460 nm with the color changing from blue to yellow. A nucleophilic addition of HSO_3^- to the C=C of coumarin ring in NIR-OH took place, and the fluorescence emission of NIR-OH (10 μM) at 664 nm gradually decreased while a new emission appeared at 550 nm (Figure S12). The emission ratio (F550/F664) showed a good linear relationship to the concentration of HSO_3^- (R^2=0.9923) (Figure S13). The detection limit was calculated to be 3.7 nM which far below endogenous SO_2 concentration (0-9.85 μM)[3]. Time-dependent emission change studies showed that the emission ratio of NIR-OH reached the maximum plateau within 90 s upon the addition of HSO_3^- (Figure 1B). pH effects on the emission ratio of NIR-OH to HSO_3^- were evaluated (Figure S14), and the suitable pH range for HSO_3^- detection was found to be 5-11. These results indicate that NIR-OH could be used for the real-time detection of HSO_3^- in living cells.

The responses of NIR-OH toward representative relevant species were also studied. No significant change was observed in the (F550/F664) emission ratio after it was treated with other analytes. Only with the addition of HSO_3^-, we could observe a noticeable response (Figure 1B). Furthermore, competitive experiments demonstrated that competitive species had no interference on the enhancement of (F550/F664) emission ratio (Figure S15). These results indicate that NIR-OH has an excellent selectivity for HSO_3^- over other biologically relevant species. To prove the sensing mechanism (Scheme S4), the product of NIR-OH with HSO_3^- was characterized by HR-MS and the desired peak (m/z=562.1177) was obtained (Figure S16). ^{1}H NMR titration experiment further confirmed the nucleophilic addition of sulfite to the C=C of coumarin ring (Figure S17).

Having demonstrated NIR-Cys and NIR-OH's sensing ability to Cys and SO_2 in buffers, these two compounds were then applied in cell imaging. Using the standard CCK-8 assay, NIR-Cys was found to be non-toxic (or low toxic) for cells (Figure S18). The primary location where Cys was metabolized to form SO_2 is mitochondria.[18] We first exploited intracellular location of NIR-Cys. MCF-7 cells were incubated with NIR-Cys and Mito-Tracker Green FM for co-

View Article Online
DOI: 10.1039/C8CC05418E

localization experiment (Figure S19). The images of the green and red channels overlapped well with a high Pearson's correlation of 0.9207 and overlap coefficient of 0.9119 demonstrating that NIR-Cys stains mainly in mitochondria. This may be due to the charge attraction between NIR-Cys with a positive charge and cellular mitochondrial membrane with the negative potential[19]. The results indicated that NIR-Cys could potentially imaging Cys and SO_2 in mitochondria. Secondly, we evaluated the potential ability of the probe to visualize Cys and SO_2 in living cells with multi-signal fluorescence. As shown in Figure 2a, MCF-7 cells only treated with NIR-Cys exhibited distinct fluorescence in red channel and non-fluorescence in green channel. When the cells were pretreated with NEM, and then incubated with NIR-Cys, weak fluorescence in red channel was noted (Figure 2b). When the cells were pretreated with increasing dosages of Cys and then incubated with NIR-Cys, a significant fluorescence increase in red channel was observed (Figure 2c). These results indicated that NIR-Cys could sense intracellular and endogenous Cys. As expected, when cells were pretreated with Cys and NIR-Cys, and then incubated with $NaHSO_3$, fluorescence in green channel was significantly increased and red fluorescence was gradually quenched at the same time (Figure 2d). We further investigated two-photon fluorescence imaging of NIR-Cys in living cells (Figure S20). The two-photon fluorescence imaging was consistent with the one photon fluorescence imaging. These results demonstrated that the probe was effective for imaging Cys and SO_2 in cellular environments.

Next, we evaluated the application of NIR-OH for imaging SO_2 in biological environment. As shown in Figure S21, when MGC-803 cells were incubated with NIR-OH (10 μM), strong fluorescence emission in red channel was observed and almost non-fluorescence in green channel was found. However, upon the addition of 100 μM $NaHSO_3$, red fluorescence was almost quenched and green fluorescence was distinctly increased. To further real-timely visualizing HSO_3^- of NIR-OH in living cells, time-dependent confocal images were conducted (Figure S22). The MCF-7 cells were pretreated with NIR-OH, and then incubated with $NaHSO_3$. The fluorescence emission enhanced in green channel was very obvious, and emission in red channel almost fully quenched. Above results illustrate that NIR-OH is an efficient candidate for imaging SO_2 in living cell.

Previous literature[9b, 20] reported that CDO's activity can be enhanced by high levels of Cys. This causes quick generation of SO_2. We thus wondered if NIR-Cys could monitor Cys metabolism in real time. As shown in Figure S23, time-dependent fluorescence increase in green channel and decrease in red channel were observed (0-240 min). The real time imaging process was also recorded with video (provided in SI). The results demonstrated that cysteine sulfinate pathway was induced by CDO. NIR-Cys was capable of visualizing the metabolism of Cys by multi-fluorescence signal in mitochondria of living cells.

Zebrafish is a highly valuable model for in vivo imaging[21]. We then examined the feasibility of visualizing Cys metabolism by NIR-Cys in zebrafish. As shown in Figure S24, zebrafish incubated with only NIR-Cys displayed red fluorescence and almost no fluorescence in green channel. In the negative control experiment, the NEM-pretreated zebrafish performed a much dimed fluorescence in both green and red channels. When zebrafish was pretreated with Cys and then incubated with NIR-Cys, strong fluorescence in red channel and non-fluorescence in green channel were observed. When zebrafish was further treated with $NaHSO_3$ for another 30 min, an obvious fluorescence increase in green channel and decrease in red channel were observed. These results demonstrated that NIR-Cys could detect Cys and SO_2 in live Zebrafish.

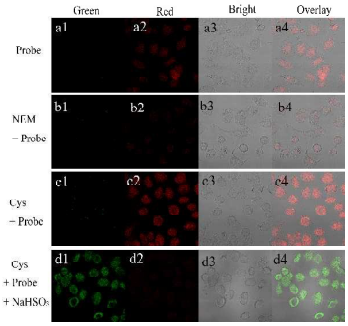

Figure 2. Fluorescent imaging of NIR-Cys responding to Cys or $NaHSO_3$ in living MCF-7 cells. Cells were incubated with (a) NIR-Cys (10 μM, 30 min); (b) NEM (500 μM, 30 min), subsequently incubated with NIR-Cys (10 μM, 30 min); (c) Cys (100 μM, 30 min), subsequently incubated with NIR-Cys (10 μM, 30 min); then incubated with $NaHSO_3$ (100 μM, 30 min) (d). (green channel of 500-590 nm, red channel of 610-700 nm)

We next tried to visualize Cys metabolism in zebrafish using NIR-Cys (Figure 3). Zebrafish was pretreated with Cys for 30 min which should accelerate Cys metabolism to produce SO_2. NIR-Cys was then loaded. A notable fluorescence decrease in red channel and a dramatic fluorescence increase in green channel were found in the following 120 min. It is the first example imaging Cys metabolism in living animals.

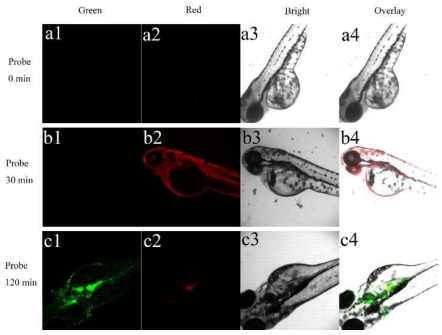

Figure 3. Confocal fluorescence images of zebrafish incubated with 10 mM of cysteine for 30 min and then treated with NIR-Cys (10 μM) for different times. (green channel of 500-590 nm with excitation 488 nm, red channel of 610-700 nm at 552 nm)

Because the fluorescence emission of NIR-Cys for Cys located in NIR region, we further examined its capability for visualizing Cys metabolism in Kunming mice. As shown in Figure 4, three mice (~20 g) were separately treated with PBS buffer (100 μL, left), NEM (100 μL, 1 mM, middle) or Cys (100 μL, 100 μM, right) via intraperitoneal injection. Then these animals were subcutaneously injected with NIR-Cys (100 μL, 10 μM). The fluorescence emission of left mouse was less significant than the emission of right mouse that was exogenous injected with Cys. Moreover, fluorescence signals in both animals reached maximum in 30 min. In contrast, negligible fluorescence emission was observed in middle mouse. We also validated NIR-OH's response to SO_2 in mice. The right mouse was

View Article Online
DOI: 10.1039/C8CC05418E

subcutaneously injected with $NaHSO_3$ (100 μL, 100 μM) for 30 min. As shown in Figure S25, the fluorescence was soon quenched in red channel, demonstrating that NIR-OH could be employed for SO_2 detection in mice.

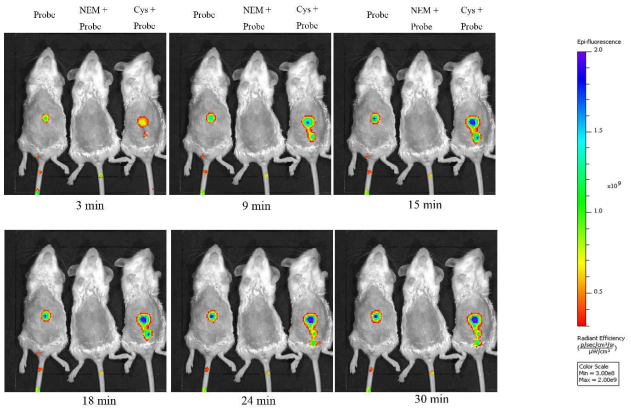

Figure 4 Fluorescent detection of Cys in living mice injected with NIR-Cys in PBS. Mice treated with PBS buffer (100 μL left), NEM (100 μL, 1 mM, middle) or Cys (100 μL, 100 μM, right) via intraperitoneal injection for 30 min. And then all the mice were subcutaneously injected probe NIR-Cys (100 μL, 10 μM). (560 nm excitation and 670 nm emission)

Finally, we applied NIR-Cys to visualize cysteine metabolism in mouse liver. 100 μL of Cys (10 mM) was intraperitoneal injected into a mouse. Another, control mouse was intraperitoneal injected with 100 μL of PBS buffer. After 4 h, liver was stained with 10 μM NIR-Cys for 30 min via intraperitoneal injected. As expected, the liver of stimulated mouse showed strong fluorescence emission. No fluorescence emission in the control liver was observed in green channel (Figure S26a). We also found that the fluorescence emission of stimulated liver was stronger than the control liver in red channel because of its high-level Cys in stimulated liver (Figure S26b).These results demonstrated the ability of NIR-Cys for Cys and SO_2 medicine screening and contribute to confirm cysteine sulfinate pathway of Cys metabolism in living animals.

In summary, we have developed a novel probe NIR-Cys for simultaneous imaging Cys and SO_2 with multi-signal fluorescence. NIR-Cys utilized the acrylate group and C=C of coumarin as the recognizing site for Cys and its metabolite SO_2, respectively. In vitro experiments showed that NIR-Cys and its Cys reaction product NIR-OH exhibit high sensitivity, excellent specificity, and fast response towards Cys or SO_2. More importantly, colocalization studies showed that NIR-Cys could specifically stain in mitochondria. Finally, the probe has been successfully employed in imaging Cys and SO_2 in zebrafish and mice. We believe that the multi-signal fluorescent probe NIR-Cys will be a useful tool to monitor Cys and SO_2 levels in living systems.

Conflicts of interest

There are no conflicts to declare.

Acknowledgements

This work was financially supported by NSFC (No. 21572209) and Program for Innovative Research Team (in Science and Technology) in University of Henan Province (No.17IRTSTHN002).

Notes and references

1 X. Chen, Y. Zhou, X. Peng and J. Yoon, *Chem. Soc. Rev.*, 2010, **39**, 2120.
2 K. Ckless, *Adv. Exp. Med. Biol.*, 2014, **806**, 301.
3 Y. Huang, C. Tang, J. Du and H. Jin, *Oxid. Med. Cell. Longev.*, 2016, **2016**, 9. https://doi.org/10.1155/2016/8961951.
4 X. B. Wang, J. B. Du and H. Cui, *Life Sci.*, 2014, **98**, 63.
5 Q. Zhang, J. Tian, Y. Bai, Z. Yang, H. Zhang and Z. Meng, *Procedia Environmental Sciences*, 2013, **18**, 43.
6 W. Xu, C. L. Teoh, J. Peng, D. Su, L. Yuan and Y. T. Chang, *Biomaterials*, 2015, **56**, 1.
7 H. Jin, Y. Wang, X. Wang, Y. Sun, C. Tang and J. Du, *Nitric Oxide*, 2013, **32**, 56.
8 T. Ubuka, J. Ohta, W.-B. Yao, T. Abe, T. Teraoka and Y. Kurozumi, *Amino Acids*, 1992, **2**, 143.
9 M. H. Stipanuk, J. J. E. Dominy, J.-I. Lee and R. M. Coloso, *J. Nutr.*, 2006, **136**, 1652S.
10 (a)Z. Yang, J. Cao, Y. He, J. H. Yang, T. Kim, X. Peng and J. S. Kim, *Chem. Soc. Rev.*, 2014, **43**, 4563; (b)B. Zhang, X. Yang, R. Zhang, Y. Liu, X. Ren, M. Xian, Y. Ye and Y. Zhao, *Anal. Chem.*, 2017, **89**, 10384.
11 (a) X. Chen, F. Wang, J. Y. Hyun, T. Wei, J. Qiang, X. Ren, I. Shin and J. Yoon, *Chem. Soc. Rev.*, 2016, **45**, 2976; (b) K. Gu, Y. Xu, H. Li, Z. Guo, S. Zhu, S. Zhu, P. Shi, T. D. James, H. Tian and W.-H. Zhu, *J. Am. Chem. Soc.*, 2016, **138**, 5334; (c) D. Zhang, W. Chen, Z. Miao, Y. Ye, Y. Zhao, S. B. King and M. Xian, *Chem. Commun.*, 2014, **50**, 4806; (d) X. Yang, Y. Liu, Y. Wu, X. Ren, D. Zhang and Y. Ye, *Sens. Actuators, B*, 2017, **253**, 488; (e) H. Xiao, P. Li, W. Zhang and B. Tang, *Chem. Sci.*, 2016, **7**, 1588.
12 (a)J. Liu, Y.-Q. Sun, Y. Huo, H. Zhang, L. Wang, P. Zhang, D. Song, Y. Shi and W. Guo, *J. Am. Chem. Soc.*, 2014, **136**, 574; (b) H. Chen, Y. Tang, M. Ren and W. Lin, *Chem. Sci.*, 2016, **7**, 1896; (c) H. Zhang, S. Xue and G. Feng, *Sens. Actuators, B*, 2016, **231**, 752; (d) Y. Qi, Y. Huang, B. Li, F. Zeng and S. Wu, *Anal. Chem.*, 2018, **90**, 1014; (e) J. Song, D. Zhang, Y. Liu, Y. Zhao and Y. Ye, *New J. Chem.*, 2015, **39**, 6284; (f) Y. Liu, K. Li, K.-X. Xie, L.-L. Li, K.-K. Yu, X. Wang and X.-Q. Yu, *Chem. Commun.*, 2016, **52**, 3430.
13 Y. Yue, F. Huo, P. Ning, Y. Zhang, J. Chao, X. Meng and C. Yin, *J. Am. Chem. Soc.*, 2017, **139**, 3181.
14 B. Xu, H. Zhou, Q. Mei, W. Tang, Y. Sun, M. Gao, C. Zhang, S. Deng and Y. Zhang, *Anal. Chem.*, 2018, **90**, 2686.
15 W. Chen, Q. Fang, D. Yang, H. Zhang, X. Song and J. Foley, *Anal. Chem.*, 2015, **87**, 609.
16 (a) W. Chen, H. Luo, X. Liu, J. W. Foley and X. Song, *Anal. Chem.*, 2016, **88**, 3638; (b) X. He, X. Wu, W. Shi and H. Ma, *Chem. Commun.*, 2016, **52**, 9410; (c) L. He, X. Yang, K. Xu and W. Lin, *Anal. Chem.*, 2017, **89**, 9567.
17 H. Wang, G. Zhou, H. Gai and X. Chen, *Chem. Commun.*, 2012, **48**, 8341.
18 E. V. Kalinina, N.N. Chernov, M. D. Novichkova, *Biochemistry Moscow*, 2014, **79**, 1562.
19 D. Cheng, Y. Pan, L. Wang, Z. Zeng, L. Yuan, X. Zhang and Y.-T. Chang, *J. Am. Chem. Soc.*, 2017, **139**, 285.
20 J. E. Dominy, L. L. Hirschberger, R. M. Coloso, M. H. Stipanuk, *Biochem J.*, 2006, **1**, 267.
21 S.-K. Ko, X. Chen, J. Yoon and I. Shin, *Chem. Soc. Rev.*, 2011, **40**, 2120.